Schulze, M.; Handge, U.A.; Rangou, S.; Lillepaerg, J.; Abetz, V.:

Thermal properties, rheology and foams of polystyrene-block-poly(4-vinylpyridine) diblock copolymers

In: Polymer (2015) Elsevier

DOI: 10.1016/j.polymer.2015.06.005

Thermal properties, rheology and foams of polystyrene-*block*-poly(4-vinylpyridine) diblock copolymers

Maria Schulze[1], Ulrich A. Handge[1,*], Sofia Rangou[1], Jelena Lillepärg[1], and Volker Abetz[1,2]

[1] *Helmholtz-Zentrum Geesthacht, Institute of Polymer Research,*
Max-Planck-Strasse 1, 21502 Geesthacht, Germany
[2] *University of Hamburg, Institute of Physical Chemistry,*
Grindelallee 117, 20146 Hamburg, Germany
** Ulrich A. Handge (Corresponding author)*
e-mail: ulrich.handge@hzg.de
Tel: +49 4152 87 2446
Fax: +49 4152 87 2499

Abstract

In this study, the thermal and rheological properties of polystyrene-*block*-poly(4-vinylpyridine) (PS-*b*-P4VP) diblock copolymers are investigated in order to get information about the optimum foaming temperature. Foams of these diblock copolymers were prepared using the technique of batch foaming with carbon dioxide as environmentally-benign blowing agent. The tailored PS-*b*-P4VP diblock copolymers with different molecular weights and a cylindrical morphology were prepared and analysed regarding their thermal stability. High-pressure differential scanning calorimetry exposes the plasticising effect of the blowing agent which yields a decrease of the glass transition temperature of the polystyrene and the poly(4-vinylpyridine) blocks. Sorption measurements were performed in order to measure the uptake of carbon dioxide in the diblock copolymer. Additionally, rheological experiments in the oscillatory mode were conducted which confirmed a microphase-separated structure of the PS-*b*-P4VP diblock copolymers by a plateau of the storage and loss moduli in the temperature range of processing. In shear and melt elongation, the transient shear viscosity and the transient elongational viscosity were much smaller than the linear viscoelastic prediction. The analysis of the foam morphology revealed that the foam density of the diblock copolymers as measured via Archimedes` principle exhibits the lowest foam density at a molecular weight in the order of 160 kg mol^{-1}.

Keywords: Polymer foams, diblock copolymers, rheology, microphase separation

1. Introduction

Block copolymers have attracted much interest as promising materials due to their ability of microphase separation. These materials combine the characteristics of thermoplastic polymers and the possibility of creating self-assembled structures on the microscopic level [1-4]. By employing the technique of living anionic polymerisation, the design of tailored block copolymers with a defined molecular weight and a small polydispersity is realisable [5-7]. Hence, block copolymers can be applied in numerous fields in industry, e.g., as insulation, absorbants or membranes [8, 9]. The covalent bonding of different types of monomers in block copolymers allows for combining different properties, e.g., for enhancing the toughness of polymers by incorporation of a soft block or for the compatibilisation of polymer blends [10-13]. In addition, the phenomenon of microphase separation enables the design of an isoporous active layer in membranes [14] and the preparation of structured cell walls in polymer foams [15]. The effect of block copolymer micelles on nucleation of foam cells in thermoplastic polymers was also explored [16]. A systematic study on the influence of blends of a styrene-*co*-acrylonitrile copolymer and a poly(2,6-dimethyl-1,4-phenylene ether) on the foaming properties was performed in Ref. [17].

New ways for fabrication of high-performance polymer foams has aroused large interest due to the wide range of applications, e.g., in membrane technology or tissue engineering [18-21]. In the field of membrane technology, new environmentally-benign methods, especially foaming of thermoplastics, are of high interest [22-24] since the common fabrication of membranes by applying the phase inversion process for polymer solutions requires a high amount of organic solvents [25, 26]. Two main methods for manufacturing polymer foams have been established: batch foaming and foam extrusion [27-29]. Generally, both processes allow the use of physical blowing agents in order to generate a cellular structure. Polystyrene has been widely used in research studies of the foam extrusion process to understand the complexity of extrusion parameters and the influence of specific polymer properties [30-33]. To achieve a homogenous and well-defined foam structure it is important to investigate and optimise the processing parameters such as foaming temperature and time [34]. A suitable candidate as blowing agent to foam polymers is carbon dioxide (CO_2) because of its environmental-friendliness and plasticisation abilities for thermoplastics combined with a reduction of viscosity [35-38].

The effect of carbon dioxide on the viscoelastic properties of the polymer can be determined by rheological measurements in shear and elongation providing information in regard with the foaming behaviour. The decrease of the steady-state viscosity of polystyrene melts caused by loading with carbon dioxide was experimentally investigated by several authors [39, 40]. Viscosity measurements in elongational flows were performed by Wang et al. [41]. In the work of Chaudhary and Jayaraman [42] rheological experiments in melt elongation and foaming of polypropylene clay nanocomposites were performed. The authors showed that an increasing degree of strain-hardening along with slower crystallization of polypropylene was associated with a smaller cell size and a larger cell density. In Ref. [43], the reduction of the transient shear viscosity and the plasticisation effect, respectively, in polystyrene melts caused by carbon dioxide was investigated. In general, homopolymers and blends of homopolymers have been studied more in depth compared to block copolymers. By way of example, polylactides showed an increase in viscosity and shear sensitivity by modifying the homopolymer through chain extenders for foam applications [44, 45]. The same effect was observed for different polypropylene homopolymers [46] and blends of them with thermoplastic olefins [47]. In addition, the influence of strain-hardening was examined which resulted in an optimised cell structure of the foams. This effect was studied in detail by Stange et al. [48] for various polypropylenes with a different molecular structure. Whereas in previous studies the relation between thermal and viscoelastic properties and foams of homopolymers has been elucidated, fundamental research on the foaming behaviour has been executed considerably less for diblock copolymers. In particular, the influence of molecular parameters (e.g., molecular weight) on the foam properties needs to be investigated further. So far, the influence of the morphology and molecular architecture of block copolymers on the viscoelastic properties has been investigated by several groups on systems such as polystyrene-*block*-poly(methyl methacrylate), polystyrene-*block*-polyisoprene or polystyrene-*block*-polyisoprene-*block*-polystyrene block copolymers [15, 49, 50].

The present study focuses on the influence of thermal and rheological properties of PS-*b*-P4VP diblock copolymers on their foaming ability. The diblock copolymers were chosen because of the high value of Flory-Huggins interaction parameter and their ability to create isoporous structures from precisely ordered and aligned morphologies in order to manufacture membranes [51, 52]. Therefore, tailored PS-*b*-P4VP diblock copolymers with number average molecular weights between 50 kg mol^{-1} and 220 kg mol^{-1} are synthesised using anionic polymerisation. Information about the thermal properties of the diblock copolymer such as thermal stability and the influence of the blowing

agent CO_2 on the glass transition temperature of the microphases is revealed. Besides, sorption measurements are performed to determine the diffusion coefficient and the uptake of carbon dioxide. These data and rheological properties are related to the foam density to reveal the influence of the molecular weight on the foaming ability and the characteristics of the foams. Additionally, the optimum foaming temperature is determined by analysing the foam density.

2. Experimental section

2.1 Synthesis of PS-*b*-P4VP diblock copolymers

PS-*b*-P4VP diblock copolymers were synthesised via sequential anionic polymerisation of styrene and 4-vinylpyridine [51, 53]. All reactants were purified by the following procedures: Tetrahydrofuran (THF) (Th. Geyer, Renningen, Germany) was successively distilled under argon atmosphere. Styrene (Sigma Aldrich, Taufkirchen, Germany) was purified with dibutyl magnesium ($MgBu_2$) and lately distilled before use. 4-vinylpyridine (Sigma Aldrich) was distilled and kept on calcium hydride (CaH_2). After purifying twice with ethylaluminum dichloride ($EtAlCl_2$), 4-vinylpyridine was distilled once again.

The reaction was carried out at -78 °C with THF as solvent and *sec*-butyl lithium (*sec*-BuLi) (Sigma Aldrich) as initiator. THF was put into the reaction vessel with lithium chloride (LiCl) (Sigma Aldrich) and stirred overnight. The first block was polymerised by adding styrene in a first and *sec*-BuLi in a second step to the solution. This was left under stirring for 4 h. After adding 4-vinylpyridine, the mixture was stirred further overnight. To terminate the reaction, the solution was quenched with purified methanol. Finally, THF was removed under reduced pressure and the polymer solution was precipitated into water before filtering and drying the obtained polymer powder.

2.2 Molecular and morphological characterisation

In order to determine the composition of the diblock copolymers, ^1H nuclear magnetic resonance spectroscopy (^1H-NMR) was carried out using a Bruker AV-300 FT-NMR spectrometer (Bruker Biospin, Rheinstetten, Germany) at 500 MHz. The solvent was deuterated chloroform ($CDCl_3$) with the internal standard tetramethylsilane (TMS).

The number and the weight average of the molar mass (M_n and M_w) and the polydispersity (*PDI*) were analysed using size exclusion chromatography (SEC). The measurement was performed at 50 °C with dimethylacetamide (DMAc) in the presence of LiCl as solvent and a flow rate of 1.0 mL min^{-1} (VWR Hitachi L2130 pump) using a pre-column and two main columns (PSS Gran 1000 Å 10 µm and PSS Gran 3000 Å 10 µm). Polystyrene standards were employed for calibration and a Shodex RI-101 refractive-index detector for analysis.

The molecular weight M_n of the diblock copolymer was calculated using the molecular weight of the polystyrene precursor and the evaluated composition of the diblock copolymers from ^{1}H-NMR data. The polydispersity *PDI* is given by the ratio of the weight average (M_w) and the number average (M_n) of the molecular weight. Furthermore, the degree of polymerisation *N* was given by the ratio of the number average (M_n) of the molecular weight and the molar mass of the monomers (M_0) for each block. The sum of both is the total degree of polymerisation *N*.

Information about the morphological structure of the diblock copolymers was obtained by transmission electron microscopy (TEM) on a FEI Tecnai G^2 F20 (FEI, Eindhoven, The Netherlands). Therefore, samples of the diblock copolymer with a cylindrical shape (preparation see Section 2.4) were cut in sections of approximately 50 nm thickness at room temperature using a Leica Ultramicrotome EM UCT (Leica Microsystems, Wetzlar, Germany) equipped with a diamond knife. The sections were stained with iodine vapour to selectively contrast the P4VP microdomains. The measurements were performed at 120 kV in bright field mode. The diameter and the distance of the centres of approximately 50 P4VP microphases were evaluated based on the micrographs.

2.3 Thermal and sorption characterisation

Information about the thermal stability of the PS-*b*-P4VP diblock copolymers was obtained by thermal gravimetric analysis (TGA) was accomplished using a TG 209 F1 Iris instrument (Netzsch, Selb, Germany). The temperature range was set from 25 °C up to 900 °C with a heating rate of 10 K min^{-1} in an argon atmosphere.

The glass transition temperature (T_g) of the PS and P4VP blocks of the diblock copolymer was analysed via differential scanning calorimetry (DSC) using a calorimeter DSC 1 (Mettler Toledo, Gießen, Germany). Approximately 7 mg of polymer were transferred into a 40 µL aluminum pan with a monoperforated lid. The heating rate was 10 K min^{-1} in a temperature range between 30 °C

and 250 °C in a nitrogen atmosphere due to the expected glass transitions of approximately 105 °C for polystyrene and 150 °C for poly(4-vinylpyridine). A heating-cooling-heating cycle was applied, and the value of T_g was determined using the second heating interval.

Besides conventional DSC, high-pressure differential scanning calorimetry (HP-DSC) was conducted on a calorimeter HP-DSC 1 (Mettler Toledo) to investigate the influence of the blowing agent carbon dioxide (CO_2) on the diblock copolymer. Therefore, approximately 7 mg of polymer were placed in a 40 µL aluminum pan with a multiple perforated lid. The measurement was carried out under CO_2-atmosphere, whereupon the CO_2-pressure was varied (1 bar, 10 bar, 20 bar). The sample was heated from 30 °C up to 250 °C at a heating rate of 10 K min^{-1} and then cooled down to 50 °C. CO_2-pressure was applied and the temperature was set isothermal at 50 °C for 2 h with a flow rate of 60 mL min^{-1} before the sample was heated up again to 250 °C under CO_2-pressure without flow. The duration of 2 h was large enough to guarantee complete saturation of the diblock copolymer powder at 50 °C. Since a single powder particle has an approximate radius of R = 200 µm and the time scale of saturation is given by $t_{sat} = R^2/D$ with the diffusion coefficient $D \approx 10^{-7}$ cm^2/s, t_{sat} roughly is 1.1 h and thus smaller than 2.0 h, see also Ref. [43].

To evaluate the uptake of CO_2 in the PS-*b*-P4VP diblock copolymers and to calculate the diffusion coefficient D, sorption measurements of CO_2 were performed using a gravimetric sorption analyzer IsoSORP® Static (Rubotherm, Bochum, Germany) [54]. The available equipment allowed determining the gas phase nonidealites, i.e. the true density, through the weighing in situ of an inert sample. The pressure accuracy was 0.006 bar. Casted and pre-dried films of PS-*b*-P4VP diblock copolymers with a thickness between approximately 250 µm and 500 µm were evacuated at 80 °C overnight to remove dissolved fluids. The sorption equilibrium data were determined at 30 °C and a pressure of 40 bar. The specific uptake of CO_2 was analysed considering gas buoyancy [55]. For the evaluation of the diffusion coefficient D, the kinetic sorption curve was fitted using the theory of Fickian diffusion for values $M_t/M_\infty < 0.6$:

$$\frac{M_t}{M_\infty} = 4\sqrt{\frac{Dt}{\pi l^2}} \tag{1}$$

where M_t is the amount of gas adsorbed in the polymer at time t, M_∞ is the mass of gas adsorbed at equilibrium ($t \rightarrow \infty$) and l is the thickness of the sample [56]. The saturation time was estimated by

t_{sat} = 0.202 l^2/D with the thickness l of the sample and the experimentally obtained value of the diffusion coefficient D [43].

2.4 Rheological measurements

To prepare samples for rheological experiments, cylindrical samples of the dried diblock copolymer were compression moulded at a temperature of 180 °C using a pillar press PW 10 H (W/O/Weber, Remshalden, Germany) to assure a defined geometry (diameter d = 8 mm, thickness h = 2 mm). In this regard, the diblock copolymer powder was prepressed at room temperature and afterwards molten at 180 °C under slight pressure for 180 s before applying vacuum for 90 s and increasing the pressure up to 45 kN for 300 s. By applying vacuum and a temperature of 180 °C during compression moulding, the remaining solvent (THF) was totally removed. The compression-moulded tablets were cooled down for at least 30 min. All samples were additionally dried in a vacuum oven at 50 °C.

The rheological measurements were performed using the rotational rheometer MCR 502 (Anton Paar, Graz, Austria) in the oscillatory mode to receive information about the viscoelastic properties of the PS-*b*-P4VP diblock copolymers. A plate-plate geometry was employed with a plate diameter of 8 mm. The gap was set slightly smaller than the thickness of the sample at room temperature (approximately 2 mm) in order to guarantee a complete contact between the plate and the sample. The experiments were carried out under nitrogen purge, with a strain amplitude γ_0 of 5% and an angular frequency ω ranging between 10^{-2} and 10^{2} rad s^{-1}. The temperature varied from 140 °C to 220 °C in steps of 20 °C. Throughout the measurements the temperature was kept constant. The experimental results were analysed using the software LSSHIFT developed by Honerkamp and Weese [57] to obtain master curves by applying the time-temperature superposition principle. To determine the region of linear viscoelasticity, amplitude sweeps were conducted in the range from γ_0 = 1% to 10% at an angular frequency ω of 10 rad s^{-1}.

Dynamic-mechanical thermal analysis (DMTA) was performed using the PS_{80}-*b*-$P4VP_{20}^{220}$ diblock copolymer with a molecular weight of 220 kg mol^{-1}. A plate-plate geometry with a plate diameter of 8 mm was applied. The measurements were carried out in the temperature range from 100 °C to 300 °C in a nitrogen atmosphere. The measurement was started at the highest temperature of 300 °C with a cooling rate of 0.5 K min^{-1}. The angular frequency was ω = 0.02 rad s^{-1} and the shear amplitude was γ_0 = 10%.

In order to investigate the behaviour of the diblock copolymer under steady shear flow, stress-growth experiments were conducted additionally using the rotational rheometer MCR 502 (Anton Paar). Therefore, the same geometry of samples and tools were used as well as working under nitrogen purge. The experiments were carried out at 220 °C, varying the shear rate from 0.1 s^{-1} to 1 s^{-1}.

The apparent elongational viscosity $\eta_{e,\mathrm{app}}$ in elongation under uniaxial loading was determined using the UXF tool (Anton Paar). Compression-moulded samples with a thickness of 0.8 mm, a width of 10.0 mm and a length of 25.0 mm were used for the investigations. The measurements were performed at a temperature of 220 °C. Three different Hencky strain rates $\dot{\varepsilon}_0$ were chosen, i.e. $\dot{\varepsilon}_0 = 0.01, 0.10 \text{ and } 1.00\ \mathrm{s}^{-1}$. The maximum Hencky strain was $\varepsilon_{\max}$=2.0 and the melting time was 8 min. The measured data in elongation were compared with the results of shear viscosity measurements (see Fig. 7) assuming a Trouton ratio of 3 (i.e. multiplication of the transient shear viscosity with a factor of 3) as well as with the linear viscoelastic prediction. The linear viscoelastic prediction was obtained by fitting a relaxation time spectrum to the data using the software NLREG [58, 59].

2.5 Preparation and characterisation of diblock copolymer foams

The technique of batch foaming was applied, where cylindrical tablets, prepared like the samples for rheological measurements, were provided into the high pressure reaction vessel highpreactor BHM-500 (Berghof, Eningen, Germany). The sorption of the diblock copolymer with the blowing agent CO_2 (Linde Gas, Pullingen, Germany, purity of 99.995%) was maintained at a gas pressure of 40 bar and a temperature of 30 °C for a loading time of 5 days. To examine the loading pressure and temperature, a BTC-3000 device (Berghof) was utilised. The foam structure was generated by a pressure drop down to ambient pressure and a contemporaneous temperature raise to the foaming temperature which varied between 90 °C and 120 °C.

After batch foaming, the vacuum dried samples were characterised with respect to the density applying Archimedes´ principle using a density determination kit (Mettler Toledo, Greifensee, Switzerland). The auxiliary liquid for the measurement was the perfluoro-compound FC-77 (3M Pharmaceuticals, St. Paul, Minnesota, USA). The density of the auxiliary liquid was calibrated before the measurements of the foams were performed.

Besides the evaluation of the foam density, scanning electron microscopy (SEM) investigations were performed using a Leo Gemini 1550 VP (Zeiss, Oberkochen, Germany) to obtain information about the distribution of the cells and their sizes as well as the characteristics of the cell wall surface. The foams were broken under cryogenic conditions and then fixed with a conductive paste on a sample holder before they were sputtered with an approximately 2 nm thick platinum coating. The cross sections of the foams were investigated at an acceleration voltage between 5 kV and 20 kV. The cell diameters were determined by converting the micrographs into black and white images and afterwards using the software analysis (Olympus) to evaluate minimum 50 cells per sample. Furthermore, the cell density N was calculated using $N = (n/A)^{3/2}$ [42] where n is the number of cells and A is a defined area of the SEM micrograph.

3. Results

3.1 Diblock copolymer characterization

The composition, the number average molecular weight M_n, the polydispersity index *PDI* and the degree of polymerisation N of the diblock copolymers are summarised in Table 1. Two groups of diblock copolymers were synthesised: The first group had a composition of 80 wt% polystyrene (PS) and 20 wt% poly-4-vinylpyridine (P4VP) with a molecular weight M_n between 50 kg mol^{-1} and 220 kg mol^{-1}, whereas the second group had a composition of approximately 77 wt% PS and 23 wt% P4VP with a molecular weight M_n between 50 kg mol^{-1} and 134 kg mol^{-1}.

Table 1. Synthesised diblock copolymers and the results of molecular characterisation.

Diblock copolymer[a]	**PS [wt%]**	**P4VP [wt%]**	***M_n* [kg mol^{-1}]**	***PDI***	***N***
PS_{80}-*b*-$P4VP_{20}$ ^{50}	80	20	50	1.05	479
PS_{80}-*b*-$P4VP_{20}$ ^{164}	80	20	164	1.06	1572
PS_{80}-*b*-$P4VP_{20}$ ^{183}	80	20	183	1.07	1754
PS_{80}-*b*-$P4VP_{20}$ ^{220}	80	20	220	1.15	2108
PS_{76}-*b*-$P4VP_{24}$ ^{50}	76	24	50	1.05	479
PS_{77}-*b*-$P4VP_{23}$ ^{106}	77	23	106	1.09	1016
PS_{78}-*b*-$P4VP_{22}$ ^{116}	78	22	115	1.08	1111
PS_{77}-*b*-$P4VP_{23}$ ^{134}	77	23	134	1.09	1284

[a] Subscript numbers indicate the weight percentage of each block and superscript numbers indicate the total number averaged molecular weight in kg mol^{-1}.

Expectedly, the polydispersity of the diblock copolymers is close to unity due to the synthesis mechanism of living anionic polymerisation which does not allow tuning the degree of polymerisation. This is indicated by a narrow distribution of the molecular weight and thus, a similar length of polymer chains for each diblock copolymer. However, the *PDI* of the diblock copolymer with the highest molecular weight of 220 kg mol^{-1} is slightly higher than the *PDI* of the other diblock copolymers.

The morphological structure of four PS-*b*-P4VP diblock copolymers with a molecular weight between 106 and 220 kg mol^{-1} was investigated by transmission electron microscopy (TEM) (Fig. 1). It was aimed to achieve diblock copolymers with a cylindrical morphology. In Fig. 1, the bright part is the PS matrix and the dark parts are the P4VP domains. The micrographs of the three diblock copolymers with molecular weights of 106, 134 and 164 kg mol^{-1} confirm a cylindrical structure without long-range order in agreement with the phase diagram of Matsen and Bates [60], whereas the diblock copolymer with the highest molecular weight created a structure on the threshold between cylindrical and spherical morphology with a stronger tendency to assembly in a cylindrical structure. The slight difference in morphology of the 220 kg mol^{-1} diblock copolymer is most probably caused by the long relaxation time. Hence the diblock copolymer had not enough time to order relax completely in an equilibrated cylindrical morphology.

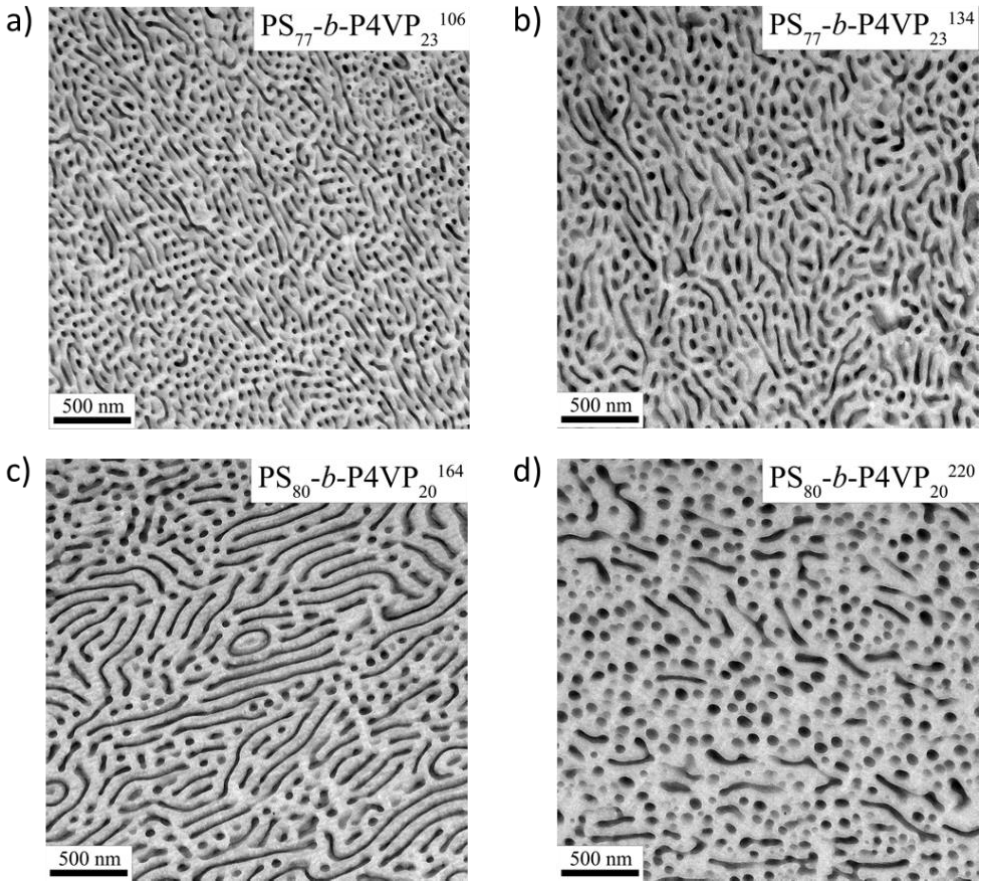

Fig. 1. Transmission electron micrographs of PS-*b*-P4VP diblock copolymers with a number average molecular weight of a) 106, b) 134, c) 164 and d) 220 kg mol^{-1}. P4VP microphases appear dark, whereas the PS microphase appears bright.

Furthermore, the analysis of the TEM micrographs proves that an increase of the molecular weight leads to larger P4VP microphases in the PS matrix. Figure 2(a) presents the average diameter of the P4VP microphases and Fig. 2(b) the distance of the centre of the P4VP microphases which were determined using the two-dimensional sections. The examined results for the diameters are 30, 42, 47 and 59 nm for the PS-*b*-P4VP diblock copolymers with a molecular weight of 106, 134, 164 and 220 kg mol^{-1}, respectively. Noticeable is the fact that the diblock copolymer with a molecular weight of 220 kg mol^{-1} has the highest deviation by the reason mentioned earlier. A similar trend is observable for the distance of the centre of the P4VP microphases. This distance (long-period) increases with the molecular weight from approximately 60 nm (M_n = 106 kg mol^{-1}) to 126 nm (M_n = 220 kg mol^{-1}).

By fitting the evaluated distances with a power-law relationship yields a power-law exponent of 0.87 ± 0.11 (Fig. 2(a)). Former studies on the relation between the diameter of the domains and the molecular weight revealed power-law exponents of 0.643 for high molecular weight diblock copolymers with a similar composition of both blocks [61] and 0.58 for cylindrical and spherical structures [62]. Additionally, the power-law relationship differs with the conformation of the polymer chains. It was found that highly entangled polymer chains have a power-law exponent of 1/3 whereas elongated polymer chains have a power-law exponent of 1 [62].

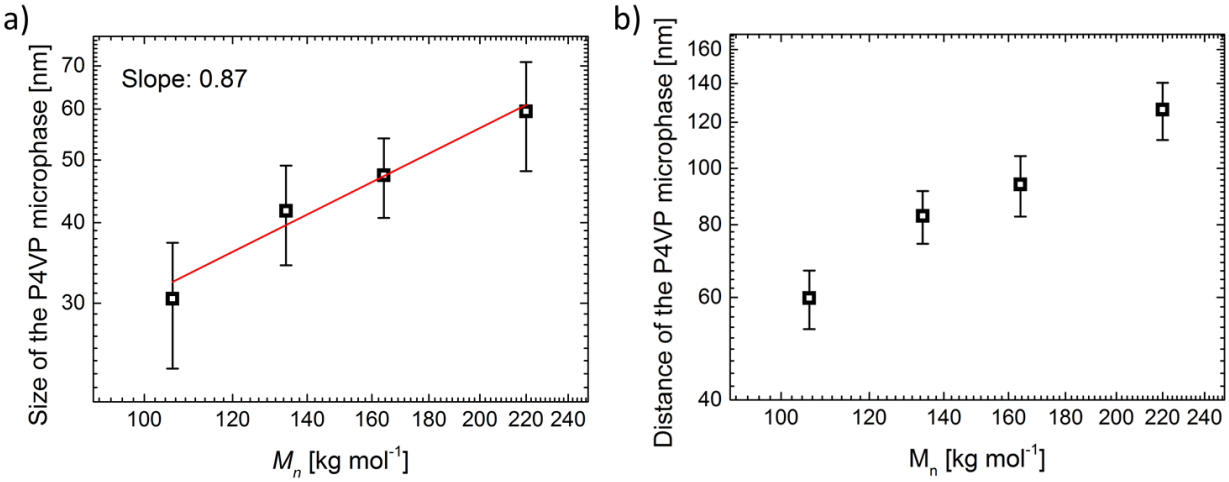

Fig. 2. a) Diameter of the P4VP microphases in the PS matrix and b) distance of the centre of P4VP microphases as a function of the molecular weight of the diblock copolymer determined by analysis of the two-dimensional ultrathin sections.

3.2 Thermal behaviour and sorption properties

The synthesised diblock copolymers were analysed using thermal gravimetric analysis (TGA) in order to get information about the stability and the suitable processing parameters for foaming. In general, the PS-*b*-P4VP diblock copolymers are stable up to 300 °C (Fig. 3). At higher temperatures, decomposition of the P4VP blocks started which was observable by a change of mass which approximately corresponds to the calculations based on the ^{1}H-NMR data. At around 400 °C, the PS microphase decomposed until the sample was completely converted into the gaseous state at 450 °C. All samples showed a change of mass of less than 3% at approximately 130 °C which may be a result of remaining water in the P4VP microphase because of its hydrophilic properties even if the samples were vacuum dried at 40 °C for at least one week before the measurement.

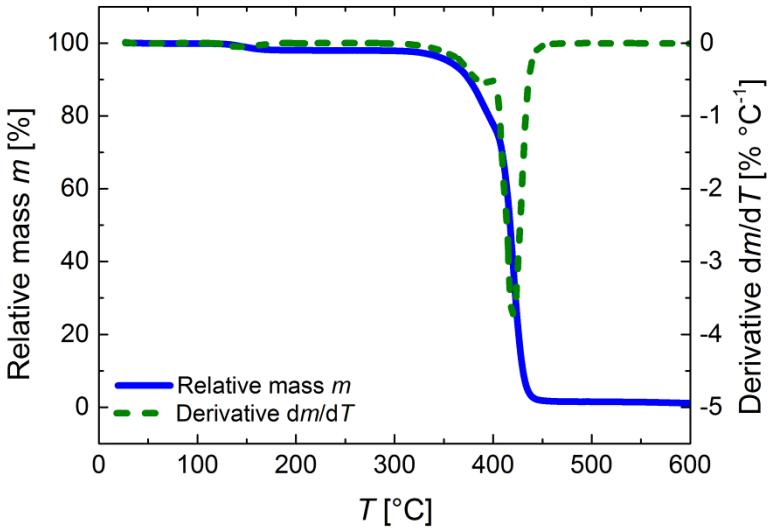

Fig. 3. TGA thermogram under inert atmosphere of a PS-*b*-P4VP diblock copolymer with a molecular weight of 164 kg mol^{-1} and its decomposition of the P4VP microphase (first step) and the PS microphase (second step). The heating rate was 10 K/min^{-1}.

The influence of the physical blowing agent CO_2 on the glass transition temperature T_g was investigated by applying conventional DSC and high-pressure DSC (HP-DSC) (Fig. 4). Three PS-*b*-P4VP diblock copolymers with molecular weights of 50, 134 and 220 kg mol^{-1} were analysed. For comparison, the data for a pristine PS homopolymer (Polystyrene PS 158K, BASF SE, Ludwigshafen, Germany, M_n = 120 kg mol^{-1}) and a pristine P4VP homopolymer (Sigma Aldrich, M_w = 60 kg mol^{-1}) is shown as well. The evaluation of the T_g for the diblock copolymers was only feasible for the PS microphase up to CO_2-pressures of 20 bar due to weak signals at higher CO_2-pressures. The glass transition temperature T_g for the P4VP microphase in the diblock copolymers was not analysable because of the lower P4VP fraction compared to the PS fraction in the diblock copolymer.

The value of T_g of the PS microphase decreased when increasing the pressure of the CO_2-atmosphere from ambient pressure to 20 bar. Considering the results, CO_2 acts as a plasticiser by causing softening of the diblock copolymers. Especially pristine PS shows this effect at which the T_g value dropped down from 105.5 °C at ambient air to 90 °C at 20 bar whereas the T_g drop for the diblock copolymers was from approximately the same T_g as the pristine PS down to around 93.5 °C for the two diblock copolymers with 20% wt% P4VP and 95 °C for the diblock copolymer with

23 wt% P4VP. At 20 bar CO_2 pressure, the value of T_g increased with the molecular weight of the diblock copolymer. Consequently, with increasing molecular weight of the diblock copolymer the plasticising effect of CO_2 is more visible [63]. The pristine P4VP showed a reduction of T_g from approximately 150 °C down to 134 °C. This information is important for the adjustment of the loading temperature in batch foaming and the optimum foaming temperature.

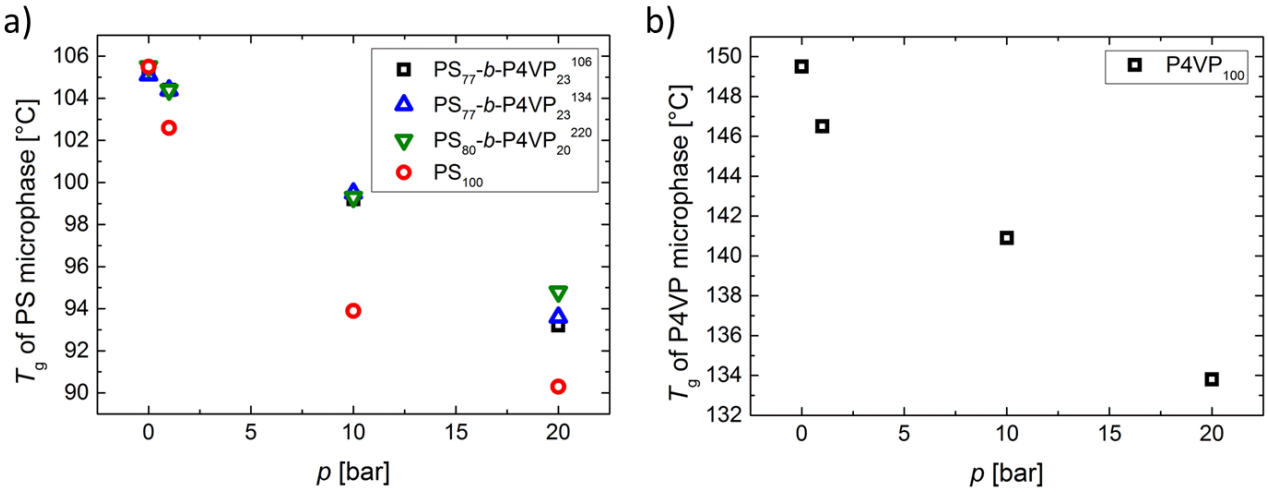

Fig. 4. Glass transition temperature T_g as a function of pressure p in a CO_2-atmosphere of a) the polystyrene microphase for three PS-*b*-P4VP diblock copolymers with molecular weights of 50, 134 and 220 kg mol^{-1} and pristine PS and b) pristine poly(4-vinylpyridine) using high-pressure DSC measurement.

The measurements with the sorption balance (see Table 2) exhibited an average specific CO_2-uptake of 6.4 wt% CO_2 in each diblock copolymer with a standard deviation of 0.15 wt% which means that the amount of dissolved CO_2 in the diblock copolymer was constant in the range of the investigated molecular weight within experimental scatter. Compared with the pure homopolymers with specific CO_2-uptakes of 5.9 wt% for PS and 7.2 wt% for P4VP, respectively, the amount of adsorbed gas results from a rule of mixture of the values of the homopolymers dependent on the composition of the diblock copolymer.

A similar trend was observable for the diffusion coefficient of the diblock copolymers since the values were all in the same magnitude between 0.45 x 10^{-7} cm² s^{-1} (M_n = 220 kg mol^{-1}) and 2.00 x 10^{-7} cm² s^{-1} (M_n = 50 kg mol^{-1}). With an increase in molecular weight of the diblock copolymer, the density of the diblock copolymer decreases due to the increase of the free volume. However, it seems

that a lower molecular weight of the diblock copolymer leads to a higher diffusion coefficient. A reason might be the faster swelling, a separation of the polymer chains initiated by the penetration of CO_2-molecules, of a low molecular weight diblock copolymer compared to high molecular weight diblock copolymer caused by the plasticization effect of CO_2 [64]. The diffusion coefficients of the pure homopolymers are in the same range of magnitude as well, 0.72×10^{-7} cm² s^{-1} for PS and 0.43×10^{-7} cm² s^{-1} for P4VP. These values correlate with the literature where the diffusion coefficients are 0.58×10^{-7} cm² s^{-1} for PS (at 25 °C) [56] and 0.13×10^{-7} cm² s^{-1} for P4VP (35 °C and 8.25 bar) [65]. The diffusion coefficient of the diblock copolymers is larger than the values for the pristine homopolymers which does not indicate the validity of a simple mixing rule for the diffusion coefficient.

The saturation time employing an average diffusion coefficient of 1.07×10^{-7} cm² s^{-1} is 21.1 h, i.e. less than one day. With regard to the evaluated saturation time, the loading time of five days for batch foaming guarantees a complete saturation of the samples.

Table 2. Specific uptake of carbon dioxide in the diblock copolymers and diffusion coefficient of the diblock copolymers at a pressure of 40 bar and a temperature of 30 °C. For comparison, measurements of pure PS and P4VP are shown.

Diblock copolymer	**Density[a] [g cm^{-3}]**	**Specific CO_2-uptake [wt%]**	**Diffusion coefficient [10^{-7} cm² s^{-1}]**
PS_{76}-*b*-$P4VP_{24}$ ^{50}	1.0967	6.21	2.00
PS_{77}-*b*-$P4VP_{23}$ ^{106}	1.0950	6.72	1.03
PS_{77}-*b*-$P4VP_{23}$ ^{134}	1.0917	6.33	1.32
PS_{80}-*b*-$P4VP_{20}$ ^{164}	1.0897	6.46	0.90
PS_{80}-*b*-$P4VP_{20}$ ^{183}	1.0883	6.45	0.45
PS_{80}-*b*-$P4VP_{20}$ ^{220}	1.0840	6.48	0.68
PS_{100} ^{120}	1.0708	5.89	0.72
$P4VP_{100}$ ^{60}	1.1884	7.18	0.43

[a] Determined via Archimedes´ principle.

3.3 Rheological properties of the diblock copolymers

The results of the DMTA measurements are presented in Fig. 5. The measurements were performed in the range from 300 °C (start temperature) to 100 °C (end temperature). Because of the plate-plate geometry, measurements at a lower temperature could not be performed due to insufficient adhesion between plates and sample. At the temperature of approximately 100 °C, the pronounced decrease of storage modulus *G′* and the maximum of the loss modulus *G″* can be anticipated which correspond to the glass transition of the polystyrene block. At higher temperatures, the dynamic moduli decrease and the rubbery plateau of the polystyrene matrix appears. In the temperature range from approximately 110 °C to 140 °C, the polystyrene microphase reacts rubbery and the poly(4-vinylpyridine) domains are in the glassy state. The maximum of *G″* at a temperature of 144 °C indicates the glass transition of the poly(4-vinylpyridine) block. At higher temperatures, *G′* and *G″* do not change with temperature. At these high temperatures, we do not observe the terminal flow regime for homopolymers (Maxwell fluid behaviour). On the contrary, the data of Fig. 5 reveal that the diblock copolymers of this work are in the microphase-separated state up to a temperature of 300 °C. This result agrees with the determination of the order-disorder transition temperature in previous studies [66].

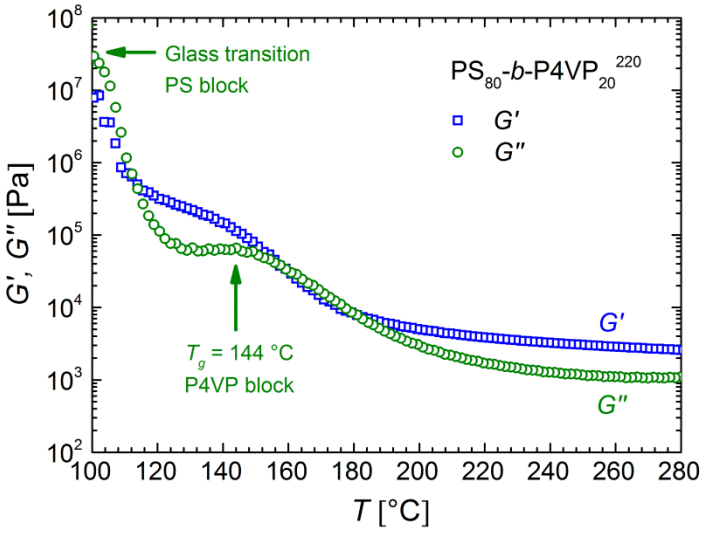

Fig. 5. Results of dynamic-mechanical thermal analysis: Storage modulus *G′* and loss modulus *G″* as a function of temperature *T* of a PS-*b*-P4VP diblock copolymer with a molecular weight of 220 kg mol^{-1}. Measurement was performed at a frequency ω of 0.02 rad s^{-1}.

Small amplitude shear oscillations were performed at several test temperatures in order to probe the frequency-dependent response of the PS-*b*-P4VP diblock copolymers of this study. Diblock copolymers consist of two different types of monomers which are associated with different time-temperature shift factors. Therefore, the time-temperature superposition principle is generally not valid for this class of polymers. However, if the shift factor for the homopolymers of these two different monomer species are approximately equal (e.g., if the glass transition temperatures of the two homopolymers are similar), then "imperfect" master curves can be created. The difference of the T_g values of both blocks is approximately 40 °C. Furthermore, since the major component polystyrene is associated with a weight fraction in the order of 80 wt% and consequently strongly influences the temperature-dependent response, the existence of such "imperfect" master curves (which mask the mismatch of the moderately different T_g values) is not surprising. Figure 6 presents the results of the application of the time-temperature superposition of two PS-*b*-P4VP diblock copolymers with different molecular weights (M_n = 50 kg mol^{-1} and 183 kg mol^{-1}). The reference temperature was 160 °C. The contribution of the rubbery plateau of the polystyrene matrix can be clearly seen. The molecular weight of the diblock copolymer strongly influences the width of this entanglement regime. At lower frequencies, a transition regime appears. At the lowest experimentally accessible frequencies the plateau caused by the phenomenon of microphase separation can be clearly seen, see also the work of Gil Haenelt et al. [49]. A close inspection of the master curve indicates that we only deal with an "imperfect" master curve such that the time-temperature superposition principle is not valid in a strict sense for this class of materials. Analysis of the data at the lowest accessible frequency indicates that a lower molecular weight of the diblock copolymers leads to a higher value of the storage modulus.

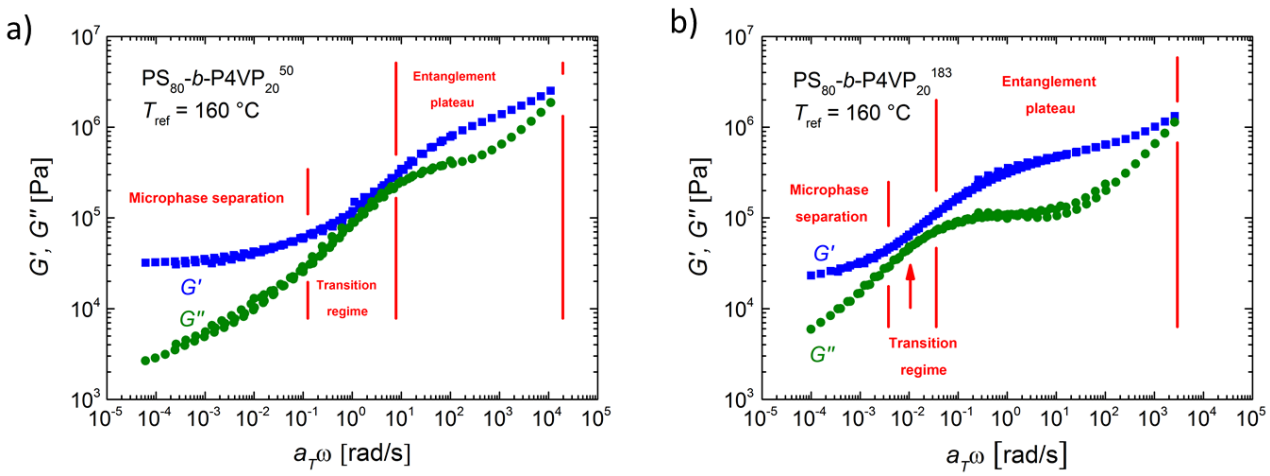

Fig. 6. Master curves of G' and G'' as a function of angular frequency ω of two different PS-*b*-P4VP diblock copolymers with molecular weights of a) 50 kg mol^{-1} and b) 183 kg mol^{-1}. The reference temperature was 160 °C and the shift factor is denoted by a_T. The entanglement plateau is mainly caused by the contribution of the PS microphase.

The frequency sweeps were performed in the linear viscoelastic regime. In order to probe the flow properties in the nonlinear range, stress-growth tests with a constant shear rate were performed. The applied shear rate varied between 0.1 s^{-1} and 1.0 s^{-1}. The data for one selected PS-*b*-P4VP diblock copolymer with a molecular weight of 134 kg mol^{-1} are shown in Fig. 7. Figure 7(a) shows the time-dependent viscosity for different shear rates. At low times, the viscosity increases with time because of the viscoelastic response of the diblock copolymers. At larger times, a steady-state value of viscosity is achieved. Figure 7(a) clearly shows that the value of the steady-state viscosity decreases with shear rate.

The influence of molecular weight on the transient viscosity is shown in Fig. 7(b). The data demonstrate that the steady-state viscosity increases with increasing molecular weight for all applied shear rates. The pronounced shear thinning at such a low shear rate of 0.1 s^{-1} (indicating a still microphase-separated morphology) suggests that the shell of polystyrene chains which are covalently bonded to the cylindrical poly(4-vinylpyridine) blocks strongly influences the value of the steady-state viscosity.

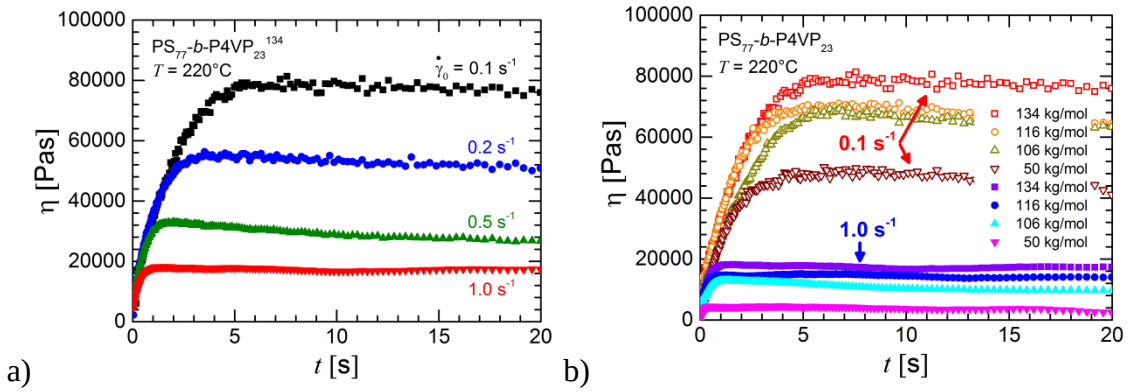

Fig. 7. Results of stress-growth tests with a constant shear rate: Transient viscosity η as a function of time t for a) a selected diblock copolymer with a molecular weight of 134 kg mol^{-1} and b) as a function of the molecular weight for two different shear rates.

The steady-state value of the viscosity as a function of shear rate is shown in Fig. 8. Two power-law functions with an exponent of -1 and -0.5 are also shown. A clear inspection of the data reveals the trend that the power-law behaviour of the stationary viscosity varies with molecular weight. At low molecular weights, the power-law exponent -1 describes the trend of the data, whereas at the largest molecular weight the power-law exponent of -0.5 corresponds to a better fit.

The rheological results in oscillatory and in steady shear can be explained in the following way, see Fig. 9. At low deformation and deformation rates, the elastic interactions caused by the microphase-separated morphology dominate. At higher stresses, the shells of polystyrene chains which are covalently bonded to the poly(4-vinylpyridine) blocks slide on each other. The size of the shell increases with molecular weight, and the interactions caused by the polystyrene chains dominate the viscous response.

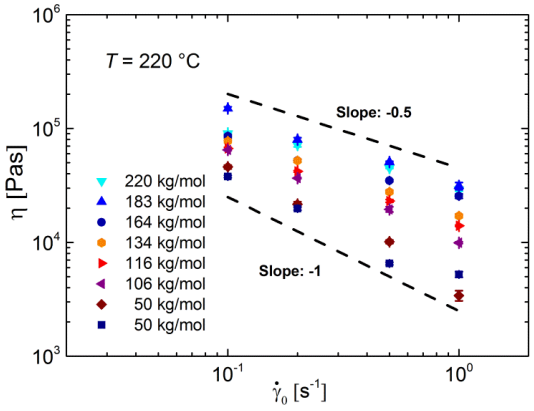

Fig. 8. Steady-state value of the shear viscosity as a function of shear rate $\dot{\gamma}_0$. The test temperature was 220 °C.

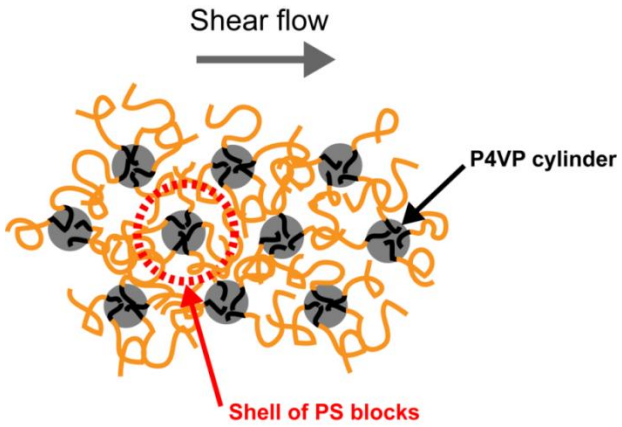

Fig. 9. Scheme of the deformation of the morphology during shear flow. The cylindrical domains of the P4VP blocks are surrounded by a shell of PS blocks. At high shear rates, the cylinders with the shell slide on each other. This deformation mechanism dominates the viscous response.

During expansion of foam cells, a biaxial elongational flow is created in the polymer shell which surrounds an expanding foam bubble. Consequently, the rheological properties in melt elongation are highly relevant for polymer foaming. Figure 10 presents the time-dependent apparent elongational viscosity $\eta_{e,\mathrm{app}}$ of two different diblock copolymers at a temperature of 220 °C. The results of the shear viscosity measurements (cf. Figure 7) which are multiplied by the Trouton ratio of 3 are also presented. Furthermore, the linear viscoelastic prediction of the elongational viscosity is shown.

The transient elongational viscosity depicts a similar trend for the diblock copolymers of this study. Because of the plateau of the storage modulus G' at low frequencies (see Fig. 6), the linear viscoelastic prediction does not lead to a steady-state elongational viscosity, but continuously increases with time in the investigated time interval. The measured shear viscosity (multiplied by a factor of 3) nearly agrees at low times with the linear viscoelastic prediction, but then achieves a constant value at larger times. The experimental data of the extensional viscosity nearly agree with the shear viscosity data up to the point of rupture in elongation. The agreement of the measured extensional and transient shear viscosity data indicate that similar morphological rearrangements take place in shear and elongation. At larger times, the transient shear viscosity and the elongational viscosity attain lower values than the linear viscoelastic prediction. In particular, the extensional

viscosity does not depict a pronounced strain hardening as observed for longchain branched polyethylenes.

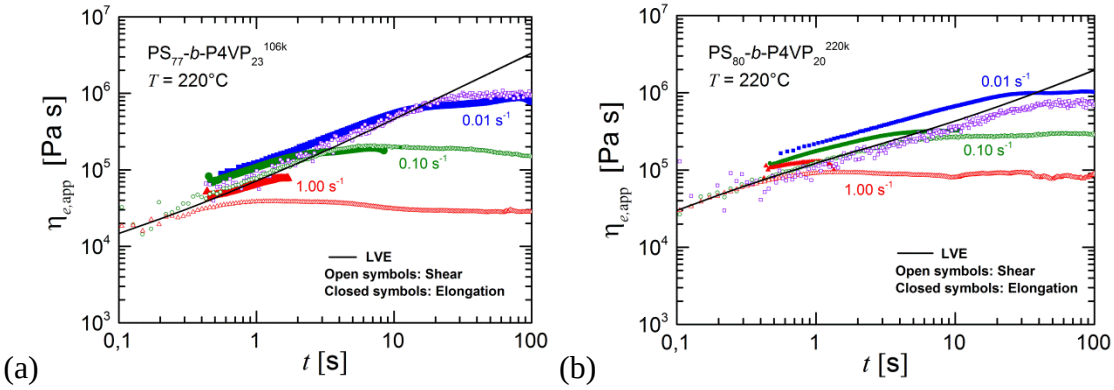

Fig. 10. Apparent elongational viscosity $\eta_{e,\mathrm{app}}$ as a function of time for three different Hencky strain rates $\dot{\varepsilon}_0$ and two diblock copolymers of this study ((a) PS_{77}-*b*-$P4VP_{23}^{106k}$ and (b) PS_{80}-*b*-$P4VP_{20}^{220k}$ diblock copolymers). The measurement temperature was 220 °C. The linear viscoelastic prediction of the elongational viscosity (LVE) and the results of the transient shear viscosity measurements (multiplied by the Trouton ratio) are also shown. The solid symbols are the data in elongation and the open symbol correspond to the shear data.

3.4 Batch foaming

The principle of the batch foaming process is illustrated in Fig. 11. Generally, batch foaming is a two-step process where the first step is the saturation of the polymer with a blowing agent (here CO_2) and the second step is the foaming of the polymer by nucleation of foam cells and expansion of the dissolved gas through pressure drop and/or increase in temperature. Therefore, the processing parameters were chosen to guarantee a saturation of the sample with CO_2 at a pressure of 40 bar provided by the gas source.

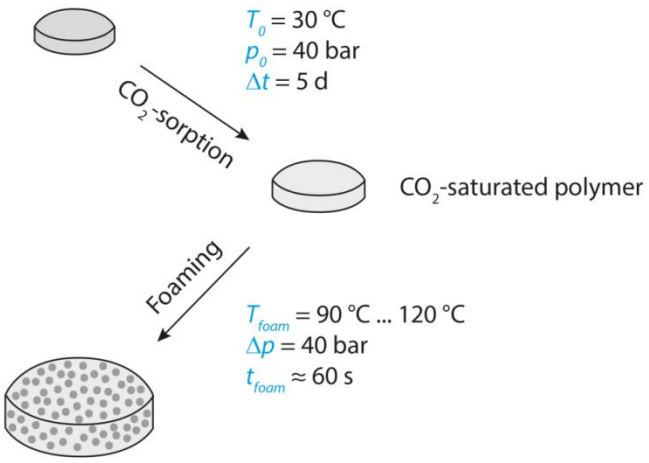

Fig. 11. Scheme of a two-step batch foaming process with the processing parameters T_0 as loading temperature, p_0 as saturation pressure, Δt as loading time, T_{foam} as foaming temperature, Δp as pressure drop down to ambient pressure and t_{foam} as foaming time.

The achieved density of the PS-*b*-P4VP diblock copolymer foams strongly depends on the foaming temperature and the molecular weight of the foamed diblock copolymers (Fig. 12). Low densities in the order of 0.15 g cm^{-3} are obtained for diblock copolymers with a high molecular weight at a foaming temperature of 110 °C. Foaming temperatures of 100 °C and 105 °C lead to relatively low densities of 0.4 g cm^{-3} down to 0.3 g cm^{-3} as well whereas diblock copolymers which were foamed below 100 °C and above 110 °C show higher densities of more than 0.4 g cm^{-3}. Especially diblock copolymers with a low molecular weight such as 50 kg mol^{-1} exhibit high densities of more than 0.7 g cm^{-3} at foaming temperatures between 90 °C and 120 °C. Consequently, at the chosen foaming temperatures a larger molecular weight yields a lower foam density. This effect can be explained as follows: A larger molecular weight leads to a larger domain spacing. At a larger molecular weight, foam cells which are nucleated in the PS microphase can grow to a larger extent without being hindered by the P4VP domains. The expanding foam cells deform the microphase-separated structure. In the case of a low molecular weight this deformation of the microstructure requires more energy.

The cell density of the foams in Fig. 12 was analysed using the scanning electron micrographs. For our experimental parameters, the cell density of the PS_{77}-*b*-$P4VP_{23}$ diblock copolymer with a molecular weight of 106 kg/mol was approximately 28.7 x 10^6 cells/cm^3. An increase of the molecular weight to 164 and 220 kg/mol led to lower cell densities of 0.5 x 10^6 and 2.0 x 10^6

cells/cm^3 for the two PS_{80}-*b*-$P4VP_{20}$ diblock copolymers, respectively. This effect is associated with the larger average diameter of the foams with a molecular weight of 164 and 220 kg/mol.

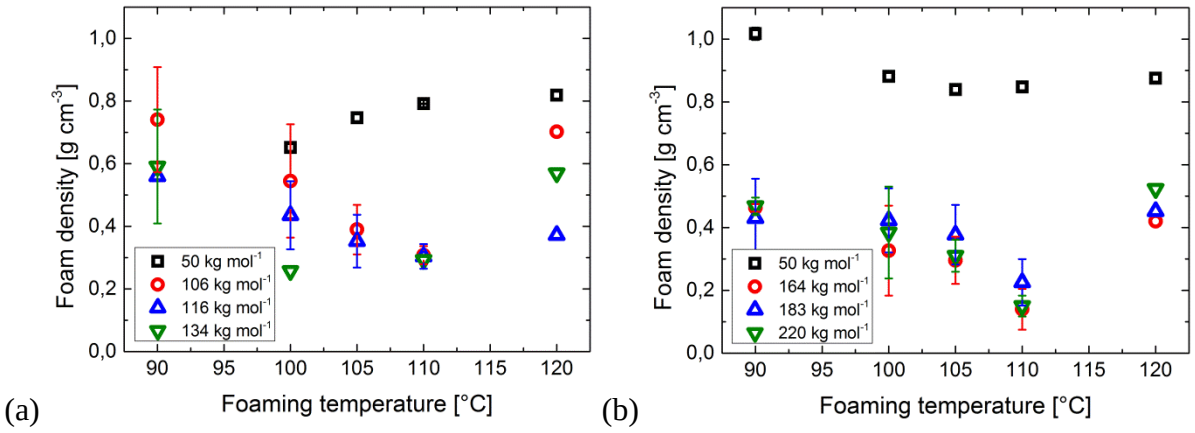

Fig. 12. Foam density of the PS-*b*-P4VP diblock copolymers as a function of the foaming temperature for the block copolymers with (a) a PS fraction of 77 wt% and (b) a PS fraction of 80 wt%. The number average M_n of the molecular weight is indicated.

Furthermore, investigations of the foam structure and the surface of the cell walls using scanning electron microscopy (SEM) give information about the quality of the foamed diblock copolymers. SEM micrographs of the foam structure (Fig. 13(b)) reveal that a foaming temperature of 110 °C led to the most regular distribution of the cells with a rather smooth surface. In contrast, the foams prepared at 100 °C and 120 °C (Fig. 13(a) and (c)) exhibit a more irregular distribution of the cells with a slightly rougher surface at 100 °C and a very rough surface at 120 °C. The high standard deviation for the samples foamed at 100 °C resulted from the combination of diffusion of CO_2 off the matrix and the high viscosity (i.e. long relaxation times of the diblock copolymer) leading to a less controllable process. The time-dependent expansion of foam cells is strongly affected by the relatively slow time-dependent increase of viscosity at low times (cf. Fig. 7) and the fast diffusion of CO_2 and consequently is strongly sensitive to fluctuations at 100 °C.

The effect of the foaming temperature on the cell structure is confirmed by evaluation of the cell size distribution of the foamed diblock copolymers. Figures 14(a) to (c) shows the cell size distribution of the PS-*b*-P4VP diblock copolymer with a molecular weight of 220 kg mol^{-1} with regard to the foaming temperature. The polymer foamed at 120 °C developed small cells (mean cell diameter d_c = 42.1 µm) with a narrow distribution whereas the polymers foamed at 100 °C and

110 °C display a broader distribution with larger mean cell diameters of 73.3 µm and 83.9 µm, respectively. The cell size distribution of the sample foamed at 100 °C is broader than the sample foamed at 110 °C. In summary, the foaming temperature influences the viscosity of the melt during expansion of foam cells.

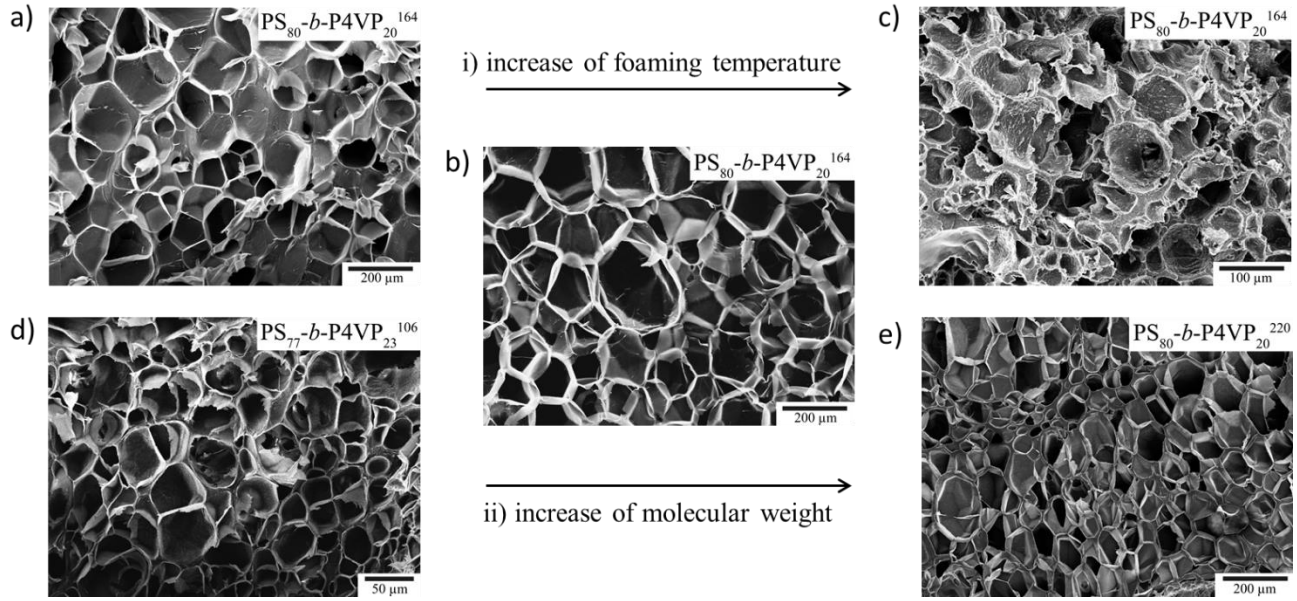

Fig. 13. Scanning electron micrographs displaying i) the influence of the foaming temperature on a 164 kg mol^{-1} PS-*b*-P4VP diblock copolymer foam with temperatures of a) 100 °C, b) 110 °C, c) 120 °C and ii) the influence of the molecular weight of PS-*b*-P4VP foams with d) 106 kg mol^{-1}, b) 164 kg mol^{-1}, e) 220 kg mol^{-1} at a foaming temperature of 110 °C.

The molecular weight of the foamed diblock copolymers led to differences in the foam structure. As seen the SEM micrographs, the diblock copolymer with a molecular weight of 164 kg mol^{-1} (Fig. 13(b)) generated on the average larger cells in contrast to the diblock copolymer with a molecular weight of 220 kg mol^{-1} (Fig. 13(e)). In contrast, the block copolymer with a molecular weight of 106 kg mol^{-1} (Fig. 13(d)) exhibited small cells. The comparison of Figs. 14(b) and (d) reveals the influence of the molecular weight at a foaming temperature of 110 °C. It is clearly seen (Fig. 14(b)) that a higher molecular weight (here 220 kg mol^{-1}) led to a more narrow cell size distribution in comparison to a broader cell size distribution of the diblock copolymer with a molecular weight of 164 kg mol^{-1} (Fig. 14(d)). Remarkably, both investigated diblock copolymers had a similar foam density at a foaming temperature of 110 °C (see Fig. 12).

Whereas the effect of foaming temperature is clearly seen by its influence on melt viscosity and foam density, the explanation of the effect of molecular weight is less obvious. Our rheological experiments in shear and elongation suggest that it is not the macroscopic viscosity which influences the final foam density, but the microrheological deformation of the cylindrical structure which appears when a gas bubble expands in the microphase separated structure. Such a microrheological analysis is beyond the scope of this study.

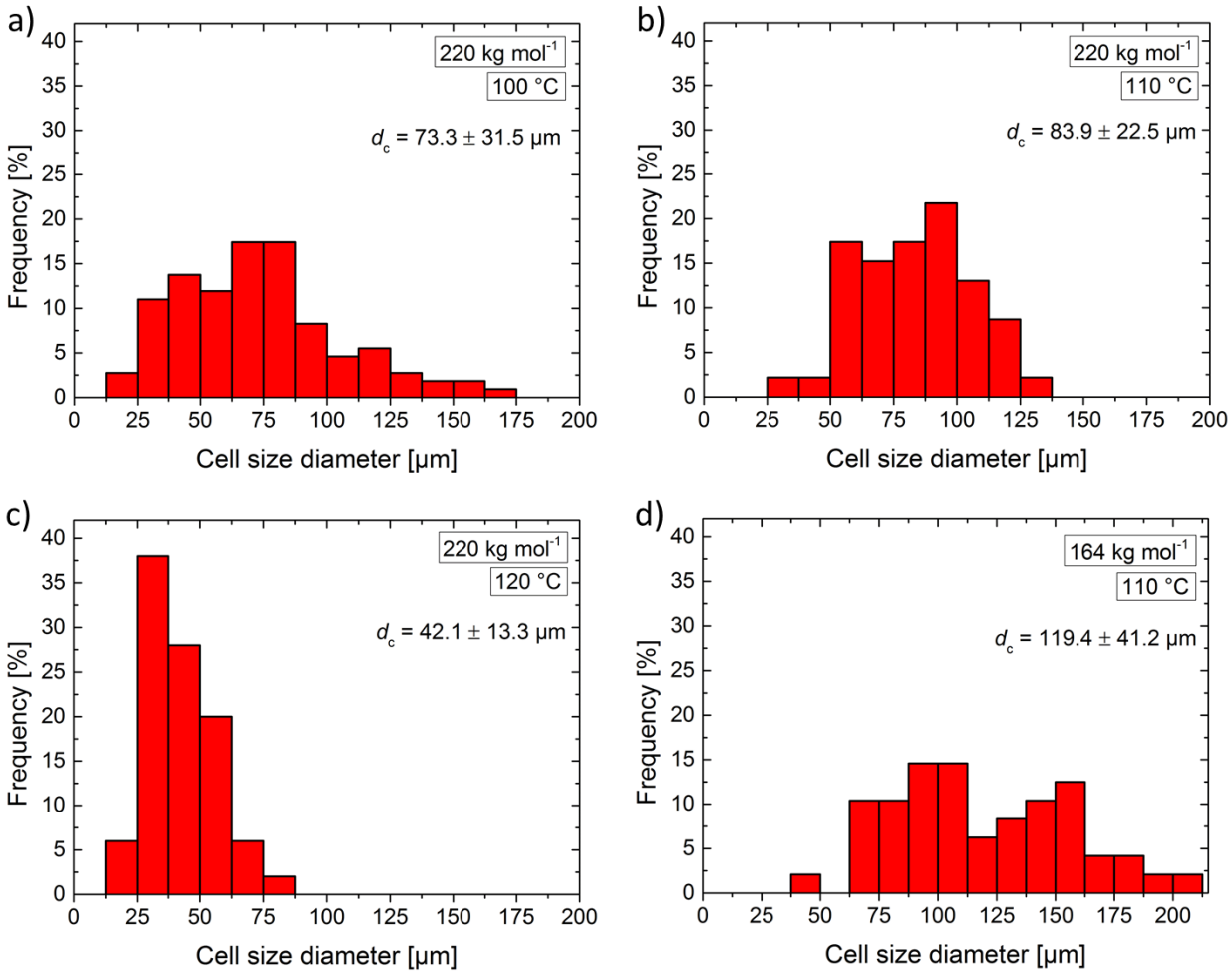

Fig. 14. Cell size distribution of PS-*b*-P4VP diblock copolymer foams with molecular weights of (a)-(c) 220 kg mol^{-1} and (d) 164 kg mol^{-1} processed at foaming temperatures between 100 °C and 120 °C indicated in the graphs. The mean cell diameter d_c and its deviation are denoted.

4. Conclusions

The present study elucidates the influence of thermal and rheological properties on the foaming behaviour of PS-*b*-P4VP diblock copolymers using CO_2 as blowing agent. The synthesis via living anionic polymerization led to diblock copolymers with defined molecular weight and composition and allows the investigation of the impact of morphology on the foaming process. DMTA experiments and transmission electron microscopy confirmed the microphase separated structure of the diblock copolymers.

The plasticising effect of CO_2 on the glass transition temperature T_g was revealed by high-pressure DSC measurements. As a result, the viscosity of the diblock copolymer is reduced which plays an important role to adjust the processing parameters of the applied foaming methods. Furthermore, sorption experiments showed an average CO_2-uptake of 6.4 wt% CO_2 at 30 °C and a pressure of 40 bar in each diblock copolymer independent of the investigated range of the molecular weight. The influence of the molecular weight on the foam structure of the diblock copolymers was observable by analysis of the foam density. The foam density decreased with higher molecular weight due to larger cell sizes determined by scanning electron microscopy. A larger molecular weight is associated with larger domain spacing and thus foam cells which are nucleated in the PS microphase can expand more easily. Besides the molecular weight, the foaming temperature played an important role in order to generate large cell structures. The optimum foaming temperature for PS-*b*-P4VP diblock copolymers of this study is 110 °C with the lowest foam density and a regular cell size distribution.

In conclusion, in spite of the microphase-separated structure diblock copolymers with a cylindrical morphology can be utilised for foam applications with similar low densities as homopolymers. The advantage of using diblock copolymers is the complexity of the system resulting in a variety of tailored properties which can be employed for the fabrication of high-performance polymer foams, e.g., insulations with water vapour permeability or isoporous membranes fabricated without the use of solvents.

Acknowledgment

The authors thank Dr. Volkan Filiz and Brigitte Lademann for the support in the synthesis of the diblock copolymers. They also thank Clarissa Abetz and Sofia Dami (scanning electron microscopy), Silvio Neumann and Thomas Emmler (nuclear magnetic spectroscopy), Maren Brinkmann (size

exclusion chromatography) and Ivonne Ternes (thermal analysis and rheological measurements) for their experimental support.

References

[1] Bates FS and Fredrickson GH. Annu Rev Phys Chem 1990;41(1):525-557.
[2] Bates FS and Fredrickson GH. Physics Today 1999;52(2):32.
[3] Abetz V and Simon PFW. Phase Behaviour and Morphologies of Block Copolymers. Block copolymers I, vol. 189: Springer, 2005. pp. 125-212.
[4] Abetz V and Boschetti-de-Fierro A. 7.02 - Block Copolymers in the Condensed State. In: Möller KM, editor. Polymer Science: A Comprehensive Reference. Amsterdam: Elsevier, 2012. pp. 3-44.
[5] Hadjichristidis N, Iatrou H, Pispas S, and Pitsikalis M. Journal of Polymer Science Part A Polymer Chemistry 2000;38(18):3211-3234.
[6] Uhrig D and Mays JW. Journal of Polymer Science Part A: Polymer Chemistry 2005;43(24):6179-6222.
[7] Ndoni S, Papadakis CM, Bates FS, and Almdal K. Review of Scientific Instruments 1995;66(2):1090-1095.
[8] Sophiea D, Klempner D, Sendijarevic V, Suthar B, and Frisch KC. Interpenetrating Polymer Networks as Energy-Absorbing Materials. In: Klempner D, Sperling LH, and Utracki LA, editors. Interpenetrating Polymer Networks, vol. 239, 1994. pp. 39-75.
[9] Stumpf M, Spörrer A, Schmidt H-W, and Altstädt V. Journal of Cellular Plastics 2011;47(6):519-534.
[10] Oommen Z, Zachariah SR, Thomas S, Groeninckx G, Moldenaers P, and Mewis J. Journal of Applied Polymer Science 2004;92(1):252-264.
[11] Adhikari R, Khatri SK, Adhikari S, Michler GH, and Calleja FJB. Macromolecular Symposia 2010;290(1):166-174.
[12] Macosko CW, Jeon HK, and Hoye TR. Progress in Polymer Science 2005;30(8–9):939-947.
[13] Ruckdäschel H, Altstädt V, and Müller AHE. Cellular Polymers 2007;26(6):367-380.
[14] Radjabian M, Koll J, Buhr K, Handge UA, and Abetz V. Polymer 2013;54(7):1803-1812.
[15] Chakkalakal GL, Abetz C, Vainio U, Handge UA, and Abetz V. Polymer 2013;54(15):3860-3873.
[16] Spitael P, Macosko CW, and McClurg RB. Macromolecules 2004;37(18):6874-6882.
[17] Ruckdäschel H, Gutmann P, Altstädt V, Schmalz H, and Müller AHE. Foaming of Microstructured and Nanostructured Polymer Blends. In: Muller AHE and Schmidt HW, editors. Complex Macromolecular Systems I, vol. 227. Berlin: Springer Berlin, 2010. pp. 199-252.
[18] Gargiulo M, Sorrentino L, and Iannace S. High performance polymeric foams. In: Acierno D, Damore A, and Grassia L, editors. IVth International Conference on Times of Polymers, vol. 1042, 2008. pp. 109-111.
[19] Krause B, Diekmann K, van der Vegt NFA, and Wessling M. Macromolecules 2002;35(5):1738-1745.
[20] Wang X, Li W, and Kumar V. Biomaterials 2006;27(9):1924-1929.
[21] Liao X, Zhang H, and He T. Journal of Nanomaterials 2012;2012:12.
[22] Huang Q, Paul D, and Seibig B. Desalination 2002;144(1–3):1-3.
[23] Krause B, van der Vegt NFA, and Wessling M. Desalination 2002;144(1–3):5-7.
[24] Abetz V. Macromolecular Rapid Communications 2015;36(1):10-22.
[25] Peinemann K-V, Abetz V, and Simon PFW. Nat Mater 2007;6(12):992-996.
[26] Lloyd DR, Kim SS, and Kinzer KE. Journal of Membrane Science 1991;64(1–2):1-11.
[27] Sauceau M, Fages J, Common A, Nikitine C, and Rodier E. Progress in Polymer Science 2011;36(6):749-766.
[28] Klotzer R, Paul D, and Seibig B. Extrusion of microcellular foams and application: Antec'97 - Plastics Saving Planet Earth, Conference Proceedings, Vols 1 - 3, 1997.
[29] Jacobs LJM, Kemmere MF, and Keurentjes JTF. Green Chemistry 2008;10(7):731-738.
[30] Han X, Koelling KW, Tomasko DL, and Lee LJ. Polymer Engineering and Science 2002;42(11):2094-2106.
[31] Zhang C, Zhu B, and Lee LJ. Polymer 2011;52(8):1847-1855.
[32] Lee K-M, Lee EK, Kim SG, Park CB, and Naguib HE. Journal of Cellular Plastics 2009;45(6):539-553.
[33] Lee M, Tzoganakis C, and Park CB. Polymer Engineering and Science 1998;38(7):1112-1120.
[34] Merlet S, Marestin C, Schiets F, Romeyer O, and Mercier R. Macromolecules 2007;40(6):2070-2078.
[35] Shieh Y-T, Su J-H, Manivannan G, Lee PHC, Sawan SP, and Dale Spall W. Journal of Applied Polymer Science 1996;59(4):695-705.
[36] Shieh Y-T, Su J-H, Manivannan G, Lee PHC, Sawan SP, and Dale Spall W. Journal of Applied Polymer Science 1996;59(4):707-717.
[37] Bortner MJ and Baird DG. Polymer 2004;45(10):3399-3412.
[38] Lee M, Tzoganakis C, and Park CB. Advances in Polymer Technology 2000;19(4):300-311.

[39] Royer JR, Gay YJ, Desimone JM, and Khan SA. Journal of Polymer Science Part B: Polymer Physics 2000;38(23):3168-3180.
[40] Wingert MJ, Shukla S, Koelling KW, Tomasko DL, and Lee LJ. Industrial & Engineering Chemistry Research 2009;48(11):5460-5471.
[41] Wang J, James DF, and Park CB. Journal of Rheology 2010;54(1):95-116.
[42] Chaudhary AK and Jayaraman K. Polymer Engineering & Science 2011;51(9):1749-1756.
[43] Handge UA and Altstädt V. Journal of Rheology 2012;56(4):743-766.
[44] Najafi N, Heuzey M-C, Carreau P, Therriault D, and Park C. Rheologica Acta 2014;53(10-11):779-790.
[45] Corre Y-M, Maazouz A, Duchet J, and Reignier J. Journal of Supercritical Fluids 2011;58(1):177-188.
[46] Xu Z, Zhang Z, Guan Y, Wei D, and Zheng A. Journal of Cellular Plastics 2013;49(4):317-334.
[47] Maani A, Naguib HE, Heuzey M-C, and Carreau PJ. Journal of Cellular Plastics 2013;49(3):223-244.
[48] Stange J and Münstedt H. Journal of Rheology (1978-present) 2006;50(6):907-923.
[49] Gil Haenelt T, Georgopanos P, Abetz C, Rangou S, Alisch D, Meyer A, Handge UA, and Abetz V. Korea-Australia Rheology Journal 2014;26(3):263-275.
[50] Han CD, Baek DM, Kim JK, and Chu SG. Polymer 1992;33(2):294-305.
[51] Rangou S, Buhr K, Filiz V, Clodt JI, Lademann B, Hahn J, Jung A, and Abetz V. Journal of Membrane Science 2014;451:266-275.
[52] Hahn J, Clodt JI, Filiz V, and Abetz V. RSC Advances 2014;4(20):10252-10260.
[53] Wode F, Tzounis L, Kirsten M, Constantinou M, Georgopanos P, Rangou S, Zafeiropoulos NE, Avgeropoulos A, and Stamm M. Polymer 2012;53(20):4438-4447.
[54] Sato Y, Takikawa T, Takishima S, and Masuoka H. Journal of Supercritical Fluids 2001;19(2):187-198.
[55] Aionicesei E, Škerget M, and Knez Ž. The Journal of Supercritical Fluids 2008;47(2):296-301.
[56] Crank J and Park GS. Diffusion in Polymers Academic Press, New York 1968.
[57] Honerkamp J and Weese J. Rheologica Acta 1993;32(1):57-64.
[58] Freiburg. Materials Research Center, Service group scientific data processing, NLREG (non-linear-regularization), Software Version May 2008.
[59] Honerkamp J and Weese J. Rheologica Acta 1993;32(1):65-73.
[60] Matsen M and Bates F. Macromolecules 1996;29(4):1091-1098.
[61] Helfand E and Wasserman ZR. Macromolecules 1976;9(6):879-888.
[62] Hoffmann VM. Die Makromolekulare Chemie 1971;144(1):309-321.
[63] Chiou JS, Barlow JW, and Paul DR. Journal of Applied Polymer Science 1985;30(6):2633-2642.
[64] Ismail AF and Lorna W. Separation and Purification Technology 2002;27(3):173-194.
[65] Shieh JJ and Chung TS. Journal of Polymer Science Part B: Polymer Physics 1999;37(20):2851-2861.
[66] Zha W, Han CD, Lee DH, Han SH, Kim JK, Kang JH, and Park C. Macromolecules 2007;40(6):2109-2119.